Sequence Specific Liquid Crystallinity in Thick Films of Model Collagen-like Polyhexapeptides

R. Valluzzi*,† and D. Kaplan*,‡

Department of Chemical and Biological Engineering and Bioengineering Center, Tufts University, Room 125, 4 Colby Street, Medford, Massachusetts 02155

Received January 20, 2003; Revised Manuscript Received March 15, 2003

ABSTRACT: To study hierarchical self-assembly of fibrous proteins, methods need to be developed to elucidate the nature of information flow between different levels of structure. The collagens present an interesting example. Sequence-dependent conformational effects are well-known in the collagen triple helix, forming a repetitive sequence (Gly-X-Y; X or Y often hydroxyproline or proline). It should thus be possible to "travel up" the structural hierarchy, and examine the features of long-range ordered structure in light of what is known about sequence and conformational relationships. The next step along this path of structural complexity is an examination of the packing of the collagen triple helices in a condensed phase and the corresponding effect of this organization on any larger domains formed. Studies of crystal structures and solid free surfaces formed by collagen peptides, slowly dried to form glassy solids with very small embedded crystallites, have been used to compare the molecular scale packing behavior of the triple helices within the longer length scale structure of the solid phase. In this instance the peptides go through a state where they are very concentrated viscous, syrupy liquids and where they form solid cholesteric-analogue phases as they dry. A qualitative correlation between the molecular packing geometry of the triple helix and the apparent chirality of the dried cholesteric phase is observed.

Introduction

The collagen proteins are present in almost every animal tissue. These proteins are composed of blocks of triple helical and "non-helical" conformations. The triple helix imparts stiffness and mechanical integrity to the molecule and may also be a major factor in the formation and morphological details of long-range ordered structures such as fibrils and helicoidal structures. Both fibrils and helicoids may have liquid crystalline origins. The triple helix is stabilized by a large proportion of the imino acids proline and hydroxyproline in the collagen triple helical sequence domains. Correlations between primary sequence, local conformation, supercoiling of the triple helix, and physical properties have been demonstrated.[1−24] The presence of amino, rather than imino acids, in the second position of the sequence (Gly-X-Y) results in a conformational change as the helix twists to accommodate hydrogen bonding between the amino acid and the environ ment.[14−16,20,22,25] With a hydrophilic or weakly hydrophobic amino acid in this position, the triple helical conformation can be destabilized. This can also occur with substitution of any amino acid for the glycine in the Gly-X-Y pattern.[14−16,20,22,25] Changes in the triple helical conformation and in supercoiling are observed as shifts in the infrared amide A band (3290−3400 cm^{-1}) position.[20,22,23,26,27] The existing research into sequence, conformation, and thermal behavior in model collagens provides a firm basis from which to address aspects of the formation of supermolecular ordered structures, such as liquid crystals and helicoid solids. Questions still remain to be addressed regarding the interplay between order and ordering phenomena such as molecular sequence, conformation, molecule−molecule packing interactions, phase behavior, and material microstructure, each of which operates at different length scales. In the current study we focus on the influence of sequence-specific conformational variations in collagen on the packing of the collagen molecules in a liquid-crystal-like phase and the effect of the pattern of amino acid side chains "decorating" the outside of the helix on its liquid crystalline (or solid-state analogue) behavior.

The collagen triple helix is known to crystallize[13,28−30] and to form liquid crystals[31] but usually occurs in biological tissues in solid analogues possessing similar orientational order but without the flow properties of a liquid.[32−42] For monodisperse chiral "rods", such as the triple helical forms of the peptides modeling the collagen molecule, cholesteric-like and chiral smectic-like materials would not be unexpected. Cholesterics and cholesteric solid analogues or pseudomorphs have been observed for collagens and reported numerous times in the literature.[40−43] Some workers have even proposed liquid crystalline intermediates in collagen fiber formation.[41,44−46] Intuitively one would expect small changes in conformation and in the overall "shape" of the helix, resulting from modifications in the primary sequence, to be transmitted into the structures formed by interhelical packing and to be observable as morphological changes in collagen-based materials. To investigate the influence of collagen molecule sequence and shape on the "twist" in collagen liquid crystalline helicoids, we have studied simple repetitive collagen-like peptides in ordered condensed phases.

Four collagen-like peptides were compared, each with a sequence based on the collagen Gly-X-Y repetitive triplet. The amino acids alanine, valine, and serine were substituted into this triplet sequence in order to probe the effects of hydrophobicity, hydrogen bonding between the amino acid and solvent, and the pattern of amino and imino acid amino acids on triple helical packing and on the corresponding morphological features observed.

† Corresponding author for physical chemistry. E-mail: regina.valluzzi@tufts.edu.

‡ Corresponding author for biochemistry. E-mail: david.kaplan@tufts.edu.

10.1021/ma0340659 CCC: $25.00
Published on Web 04/25/2003

Glassy solids prepared from the peptides were examined using X-ray diffraction analysis. Because such a large number of structural studies have been performed on model triple helical collagens in the past, assigning unit cells from the X-ray powder patterns obtained was straightforward. Banded textures were observed on the free surfaces of glassy solids prepared from the peptides using tapping mode AFM. The period of the bands in the banded texture are well correlated to the packing asymmetry, the ratio of nearest neighbor packing distances, obtained crystallographically. Although the materials are solid, defects are observed in the banded textures suggestive of a cholesteric phase.

Experimental Section

Sequence Design. Three sequences were designed to examine the effect of different amino acids in the X position of Gly-X-Y. Valine and alanine in the core repeating sequences GVPGPP and GAPGPP were used to examine amino acids of varying hydrophobicity in the X position. Valine is extremely hydrophobic. In addition, because the two methyl groups are attached directly to the β-carbon, most of the side chain volume and much of any hydrophobic shielding by the side chains are located very close to the main chain. Possible steric strain is thus exacerbated for valine as opposed to leucine or isoleucine and has been observed using computer modeling in a previous study.[9] Serine in the core repetitive sequence GSPGPP was selected because, like valine and alanine, it is also a small amino acid. However serine is hydrophilic and possesses a mobile side chain that can hydrogen bond to the solvent (water). The interaction between water and the triple helical peptide based on GSPGPP will thus be very different near the serine side chains than elsewhere along the chain and may amplify the effective chirality of the helix.

One additional sequence based on a core GAPGPA repetitive sequence was used to explore the effect of different patterns of substituted amino acids.

Peptide Preparation. Four peptides with collagen-like repetitive sequences were prepared using standard Fmoc synthesis (Tufts University Core Protein Facility, Boston): $(E)_5(GAPGPP)_6(E)_5$ (**1**); $(E)_5(GVPGPP)(E)_5$ (**2**); $(E)_5(GSPGPP)_6(E)_5$ (**3**); $(E)_5$ $(GAPGPA)_6(E)_5$ (**4**).

The peptides were desalted and HPLC purified, and mass spectrometry was used to verify the mass and sequence of each peptide.

The lyophilized peptides were soluble in deionized (18 MΩ, Millipore filtration system) pure water at concentrations up to 100 mg/mL. Solutions were prepared in pure deionized water at a concentration of 40 mg/mL for each peptide. Then 100 μL of each peptide solution was placed into separate wells of a polystyrene (uncoated) tissue culture well. The solutions were then placed into a refrigerator and dried at 3 °C over 3 days. The close spatial proximity of the solutions in the well plate and the simultaneous sample preparation were used to ensure that conditions experienced by each peptide solution during drying would be identical.

Characterization. The peptides were characterized using FTIR (Bruker Equinox 55) to obtain transmission spectra for the solid glassy films obtained after drying. Spectra were converted to Kubelka−Munk units using an algorithm provided by the manufacturer. No further manipulation was needed. CD spectra were obtained using a JASCO CD spectrometer with dry nitrogen purge, for dilute aqueous solutions of the peptides ranging from 5 to 40 mg/mL in pure water over temperatures ranging from 2 °C to ambient temperature.

X-ray diffraction on the same glassy films was carried out at the MRSEC X-ray central facility at the University of Massachusetts, Amherst, MA. Fujifilm image plates were used to acquire the X-ray diffraction patterns.

Polarizing light microscopy was used to verify a cholesteric texture in the films of dried peptide. Atomic force microscopy and environmental scanning electron microscopy were used to characterize the free surfaces of the dried peptides. A Digital Nanoscope atomic force microscope was used in contact and noncontact tapping mode to obtain phase images of the surfaces (contact) and to image the topography of the surfaces and adsorbed hydration water (noncontact and contact). Smooth glass surfaces were scanned under the same conditions to verify that the patterns observed were not a tapping mode sample reflection artifact. The phase images contain viscoelastic information about the sample.

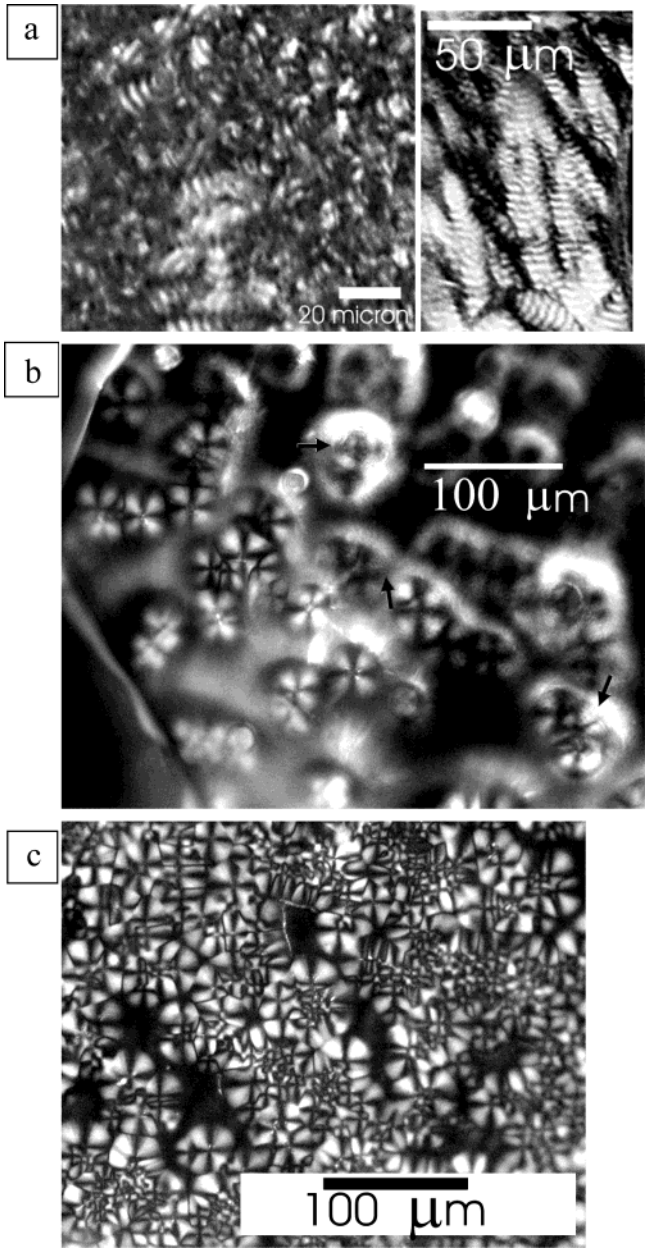

Figure 1. Polarizing optical microscope data obtained from dried peptide films. Preparation of thick (roughly $^1/_2$ mm) films for corroboration in X-ray diffraction results in smearing of the images from out of focus planes in the material. However characteristic optical textures can still be observed. (a) Left: Cholesteric spherulite texture from peptide **4** ("GAPGPA"). Right: Focal conic cholesteric texture from peptide **1** ("GAPGPP"). (b) Film from peptide **3** ("GSPGPP"), where a fine sinusoidal texture is observed in the surface skin above the prominent birefringent features (*arrows*). (c) Overall bulk texture observed for peptide **3**, which is a smectic polygon texture, shown here by focusing on the interior of the film.

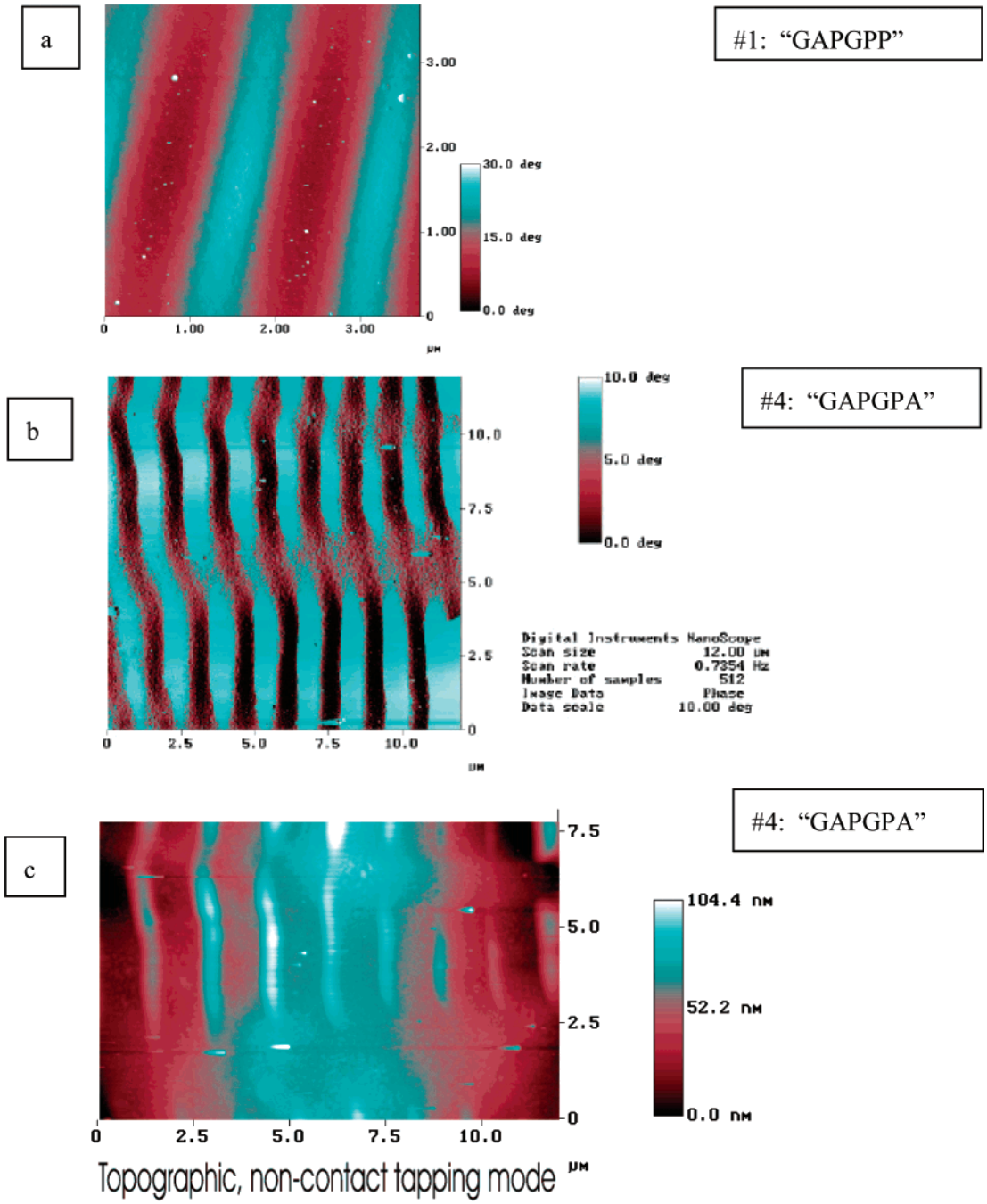

Figure 2. AFM images of the free surfaces of the peptide films (the side exposed to air while drying). (a) AFM contact tapping mode images of peptide **1** ("GAPGPP"). The tapping phase lag image indicates sinusoidal modulations in surface viscoelasticity. (b) Contact tapping mode image of peptide **3** ("GSPGPP"), again using phase contrast to image surface viscoelasticity. (c) Noncontact tapping mode image of a section of the sample in part b. Well-defined bands of adsorbed water are observed on top of the softer (more viscous) bands of the sinusoidal texture in the material. These observations suggest a sinusoidal alternation of more viscous hydrophilic and elastic hydrophobic banded regions at the surfaces of the materials.

Results and Analysis

Polarizing Microscopy. Banded cholesteric and cholesteric focal conic textures were observed for all of the peptide materials except those from the serine substituted sequence, peptide **3**. An example of a typical cholesteric polarizing optical microscopy texture shown in Figure 1a for peptide **1**. For peptide **3**, sinusoidal features typical of cholesteric orientation were only observed in a thin surface layer. These features can be observed in the optical microscope by focusing on the top surface of the films, as seen in Figure 1b. The bulk portion of these materials formed a smectic polygon texture, shown in Figure 1c. Differences in drying time affect the structural organization of the collagen peptides, suggesting that faster drying trapped a cholesteric structure at the surface of peptide **3**.

AFM. All of the free surfaces of peptides dried in the cell culture plate examined (3 days drying time) had banded patterns evident in contact tapping mode phase images (Figure 2a). In many cases, topographic features corroborate the phase images (Figure 2, parts b and c). Topographic images can be obtained reproducibly in noncontact tapping mode for these samples. Contact mode tapping alters the surface being examined, indi-

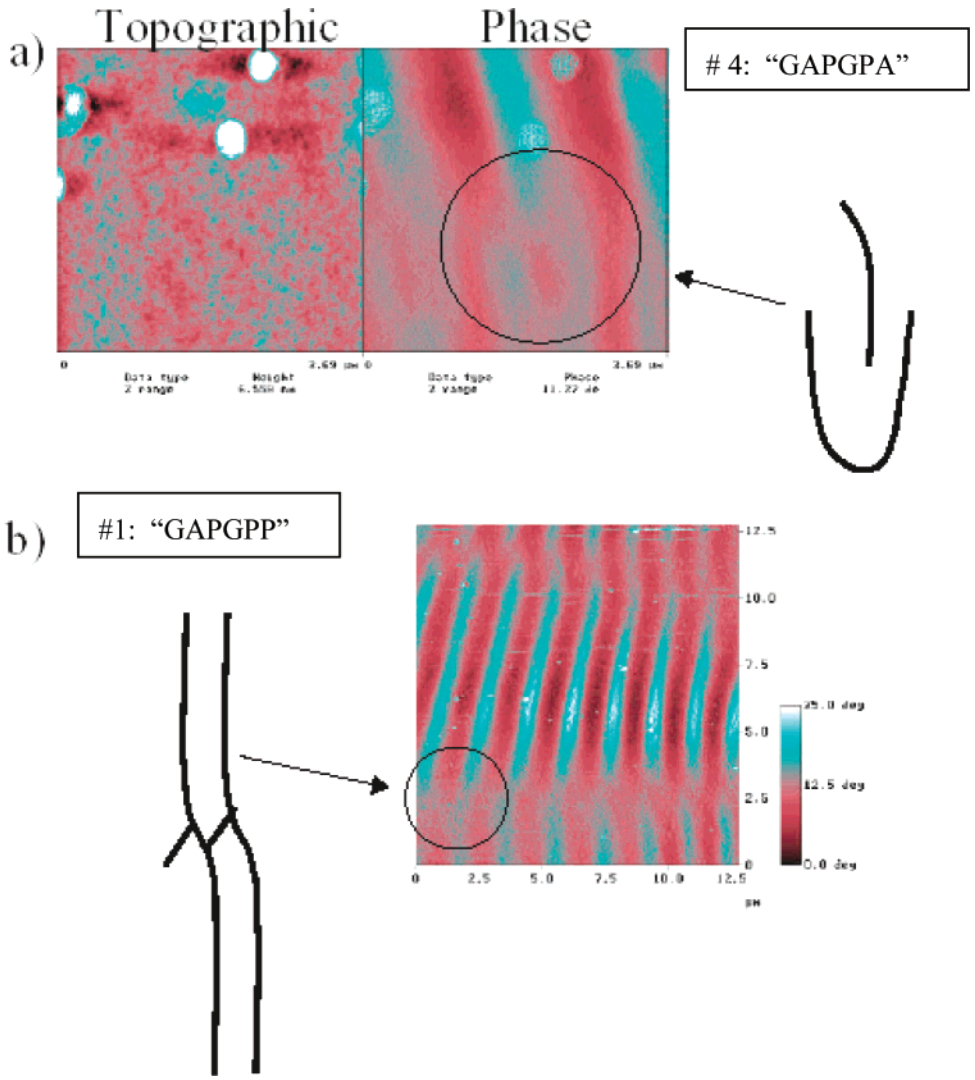

Figure 3. Defects similar to those observed in cholesteric "fingerprint" textures observed in AFM images obtained using viscoelastic contrast in tapping mode. (a) Peptide **4** ("GAPGPA"). The topographic image at the left indicates a smooth surface, but the phase image (viscoelastic contrast) at the right reveals a row of grain boundary defects. (b) Peptide **1** ("GAPGPP"). Here the texture twists into the film and the bands split.

cating very soft or liquid material forming the bands of topographic contrast (the high features) on the surface. When the phase images are viewed these same bands have a phase lag of 15−30°, indicating a viscous component to the response of the surface to the tip. In several instances, defects in the banded pattern appear. The most typical defects observed are regions where two mismatched banded grains meet (arrow in Figure 3a). In other peptide surfaces the pattern appears to periodically bend (Figure 3b). Criss-crossed patterns are typically observed for peptide **3** ("GSPGPP") and in some areas on the peptide **1** ("GAPGPP") surface (Figure 4, parts a and b). These appear at first glance to be two patterns simply superimposed, perhaps as thin superimposed layers. Close examination reveals that the pattern is "smeared out" at the points where two bands cross suggesting that the two patterns are connected—perhaps in grain boundary defects. This texture suggests that the peptide is entering a TGB phase.[47] In addition the angles between the crossed bands are different for the two peptides exhibiting the defect. The AFM phase and topographic data in tapping mode clearly correlate the raised portions of the surface (noncontact mode) with the areas that have the highest loss component in their viscoelastic response (contact mode). In noncontact mode, these same regions are easily modified by the tip, suggesting a liquid such as adsorbed water. The architecture of the peptides used in the study easily accounts for the pattern of raised, soft, hydrophilic bands on the surface of the material. Each sequence used contains a relatively hydrophobic triple-helix generating core region (36 amino acids), which in the triple helical conformation would also be dense and stiff. Glutamic acid blocks, too bulky to fully participate in the triple helix, were added to the ends of each peptide to aid in solubility. These regions are extremely hydrophilic, and are expected to be less stiff than the triple helical portions of the peptide. If the hydrophilic end groups are periodically buried and then exposed in a pattern of changing helical orientations at the solid surface, comparable to a cholesteric orientation as shown in Figure 5, a pattern of sinusoidal stiff hydrophobic and wet raised (from water and swelling) softer hydrophilic bands would be expected throughout the material.

X-ray Diffraction. When the solid sample of material used in AFM was used to obtain X-ray diffraction patterns, powder patterns were observed for all five

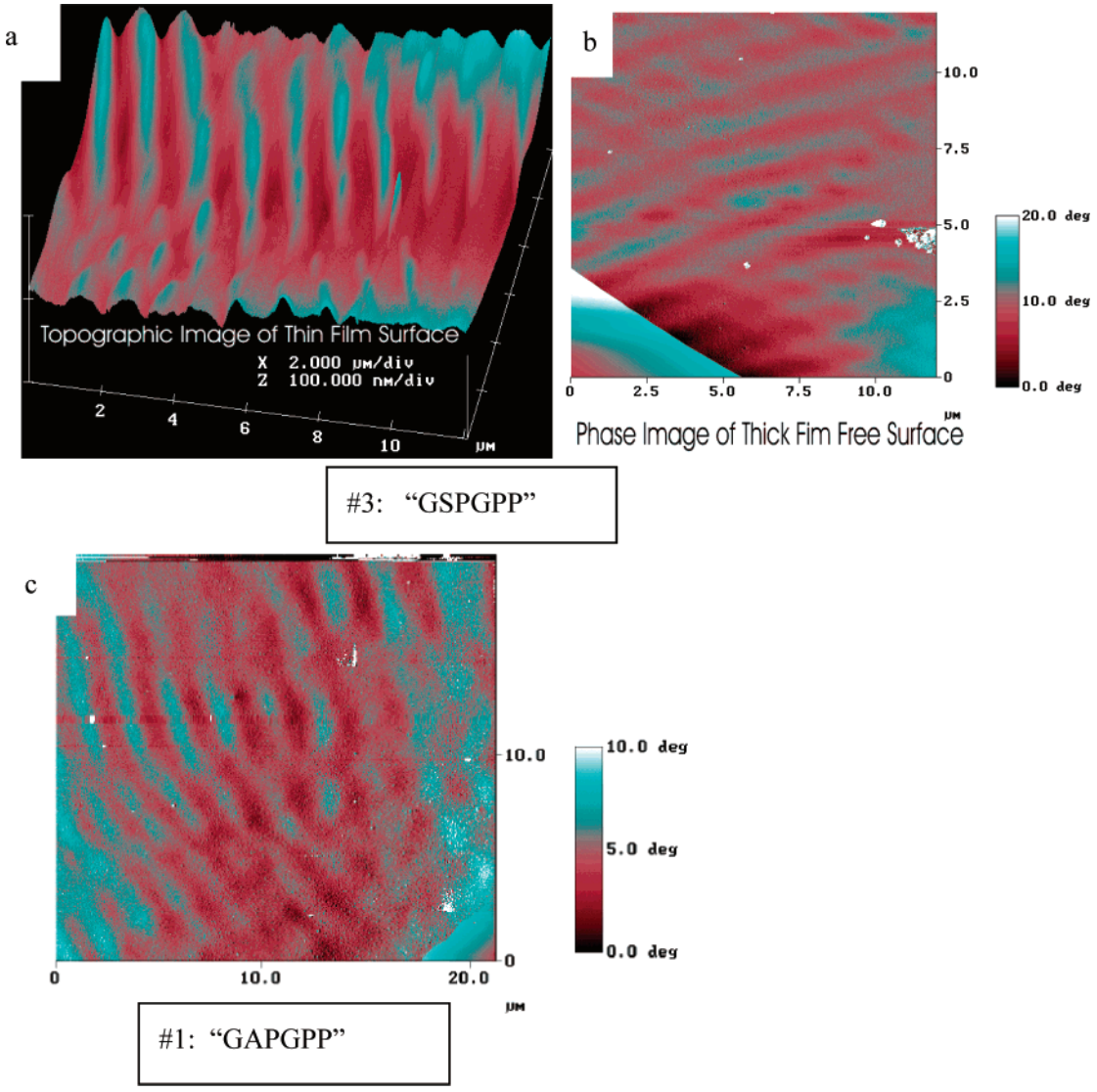

Figure 4. TGB-like defect patterns in the surface viscoelasticity patterns on the peptide materials imaged using tapping mode AFM. (a) In this thin film topographic image, peptide **3** ("GSPGPP") has a surface pattern of criss-crossed bands meeting at angles of approximately 60 and 120°, which define a space-filling translationally periodic grid or mesh. This pattern suggests a defect phase such as one of the TGB phases. (b) A phase mode image confirms a pattern of varying viscoelasticity is present, and is associated with the topographic features. (c) A criss-cross pattern obtained for peptide **1** ("GAPGPP") has angles of predominantly 90° between crossing bands in the defect texture. This is again a space-filling periodic texture, suggestive of a TGB phase.

peptides. All of the powder patterns contained recognizable collagen-like features including strong lower angle reflections at 10−13 Å, representing inter-triple helical packing dimensions, and a clear reflection at 2.67 or 2.95 Å (depending on which triple helix conformation is observed) corresponding to known rise per amino acid values for *different* stable conformations of the collagen triple helix. Since the conformation and crystal structures are known for many collagen-like peptides and polypeptides initial assignment of unit cell parameters was straightforward. The unit cells, observed and calculated *d*-spacings, and observed relative intensities can be found in Tables 1−4 for peptides **1**−**4**, respectively.

Spectroscopy. FTIR spectra were obtained for the solid material used in the X-ray and AFM analysis. The conformation of each strand in the collagen triple helix is very similar to the conformation of a polyproline II helix. In the stretched collagen structure first reported by Rich and Crick, the collagen triple helix makes 3 turns in 10 amino acids with a rise per amino acid of 2.95 Å (other, less extended triple helices can have a 2.67 or 2.87 rise per amino acid).[13] The polyproline II helix makes 1 turn in 3 amino acids(or 3 in 9) and has a rise per amino acid of 3.06−3.12 Å. Thus, the differences in the amide I region of the spectrum, which is conformationally sensitive, are expected to be subtle. The amide A band, which is sensitive to changes in hydrogen bonding, is sometimes cited as a more sensitive measure of collagen triple helix formation and conformation or "degree of supercoiling".[23] Spectra from the solid peptide materials all had amide A absorbances near 3300 cm^{-1}, indicating triple helical structure.[9] As can be seen in Figure 6, multiple absorbance bands were observed for the peptides in the amide A region, with three absorbance bands occurring between 2900 and 3100 cm^{-1}. These bands are in the same locations for all of the peptides. Two additional bands appear bracketing this range. A high-frequency band occurs between 3150 and 3250 cm^{-1}, with slightly different values for the four peptides. This band is markedly sharper and stronger and is also shifted to the highest frequency for

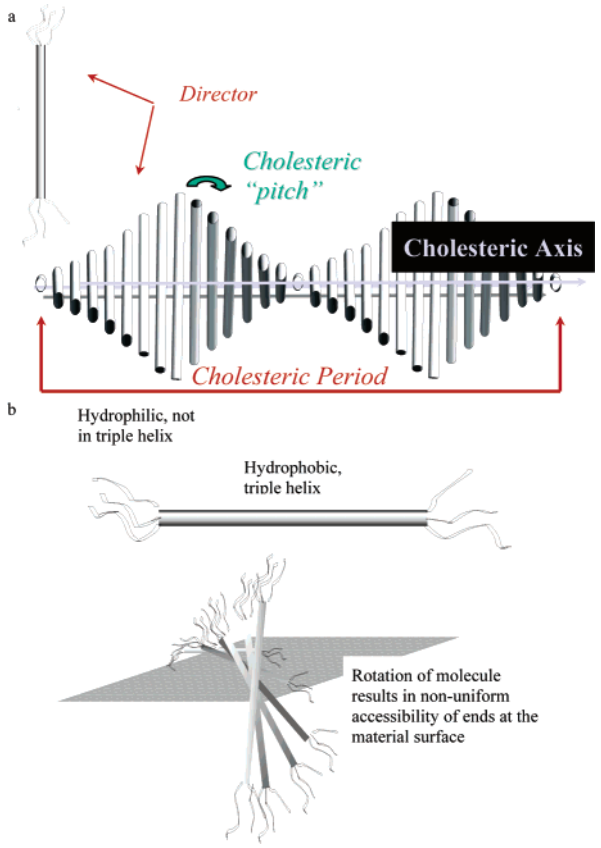

Figure 5. Orientation of the collagen triple helices within the material explains the observed film surface features. (a) In a cholesteric phase or a solid analogue, the collagen rods will align with each other locally, but the average orientation of the molecules will twist as one moves through the material. (b) Each collagen peptide was designed with a triple helix forming core sequence (36 amino acids, repeating Gly-X_1-Y_1-Gly-X_2-Y_2 hexapeptides) and five amino acid long glutamic acid solubilizing blocks at the ends—a rigid hydrophobic rod capped with hydrophilic soft ends. As these rods twist, the soft hydrophilic end blocks are periodically forced to the surface.

Table 1. X-ray Diffraction Rings Observed for Peptide 1 ("GAPGPP"), Indexed on a Hexagonal Unit Cell[a]

d_{obsd}	index	d_{calcd}
12.64	1 0 0	12.64
7.63	1 0 1	8.18
	1 1 0	7.30
4.29	2 1 1	4.36
	1 1 2	4.32
2.67	0 0 4	2.67

[a] Peptide **1** "GAPGPP" Glu_5 (Gly-Ala-Pro-Gly-Pro-Pro)$_6$ Glu_5. Hexagonal; a= 14.6 Å; c=10.7 Å. Single chain, 4-fold helix.

peptide **1** ("GAPGPP"), the peptide with the shortest rise per amino acid in X-ray patterns and a distinct collagen triple helical conformation. There is also a low-frequency band that occurs between 2850 and 2900 cm^{-1}. This band also has different frequencies for the different peptides, but peptides with higher frequencies in the 3150−3250 cm^{-1} region have lower frequencies in the 2850−2900 cm^{-1} region. Small differences in amide I band frequencies are also observed for the four peptides, but are difficult to interpret. Absorbance bands are observed for all of the peptides at approximately 1630 and 1650 cm^{-1} in the amide I region, where the 1650 cm^{-1} band was strongest for peptide **1** ("GAPGPP"). While a detailed analysis of the spectroscopic data are beyond the scope of this study, the observed changes in the conformationally sensitive amide A and amide I bands suggest that there may be small changes in the degree of supercoiling for peptides **2**, **3**, and **4** (while peptide **1** is in a distinct conformation).

Table 2. X-ray Diffraction Rings Observed for Peptide 2 ("GVPGPP"), Indexed on a Two-Chain Orthorhombic Unit Cell[a]

d_{obsd}	index	d_{calcd}
12.15	1 0 0	12.15
9.81	1 1 0	9.82
4.91	1 3 0	5.06
	0 3 3	4.84
3.94	0 7 1	4.09
	0 4 3	3.84
2.95	0 0 10	2.95

[a] Peptide **2** "GVPGPP" Glu_5 (Gly-Val-Pro-Gly-Pro-Pro)$_6$ Glu_5. Orthorhombic; a = 12.2 Å; b = 16.7 Å; c = 29.5 Å. Two chains, 3.3-fold helices (10/3).

Table 3. X-ray Diffraction Rings Observed for Peptide 3 ("GSPGPP"), Indexed on a Two-Chain Orthorhombic Unit Cell[a]

d_{obsd}	index	d_{calcd}
12.21	1 0 0	12.15
4.74	0 3 3	4.77
3.90	3 1 0	3.93
	1 1 7	3.85
2.93	0 0 10	2.95

[a] Peptide **3** GSPGPP Glu_5 (Gly-Ser-Pro-Gly-Pro-Pro)$_6$ Glu_5. Orthorhombic; a = 13.8 Å; b = 16.4 Å; c = 29.5 Å. Two chains, 3.3-fold helices (10/3).

Table 4. X-ray Diffraction Rings Observed for Peptide 4 ("GAPGPA"), Indexed on a Two-Chain Orthorhombic Unit Cell[a]

d_{obsd}	index	d_{calcd}
10.53	1 0 0	10.54
8.46	0 1 3	8.45
5.55	0 3 0	5.50
4.77	0 2 5	4.80
4.10	0 1 7	4.08
3.42	3 0 3	3.31
2.95	0 0 10	2.95

[a] Peptide **4** "GAPGPA" Glu_5 (Gly-Ala-Pro-Gly-Pro-Ala)$_6$ Glu_5. Orthorhombic; a = 10.53 Å; b = 16.5 Å; c = 29.5 Å. Two chains, 3.3-fold helices (10/3).

CD spectra obtained for the peptides in solutions with concentrations ranging from 5 to 40 mg/mL and at temperatures ranging from 2 °C to ambient temperature did not indicate that the triple helix was present in that range of solution concentrations. Similar differences between solid and solution state collagen secondary structure have been observed previously and suggest that triple helix formation may be concentration dependent.[14−16] Concentration-dependent triple helix melting temperatures have been confirmed in recent studies by Goodman et al.[6,7]

Discussion

The peptides observed had sinusoidal textures on their surfaces which are similar to those characteristic of cholesteric mesophases, but were solid materials. The hydrophilic/hydrophobic "barbell" architecture of the peptides (Figure 5) would result in the pattern of soft hydrophilic (wet) and stiff hydrophobic bands observed if the orientation of the triple helical molecules was rotating in a manner analogous to a cholesteric. The free surfaces of the solid materials are extremely smooth,

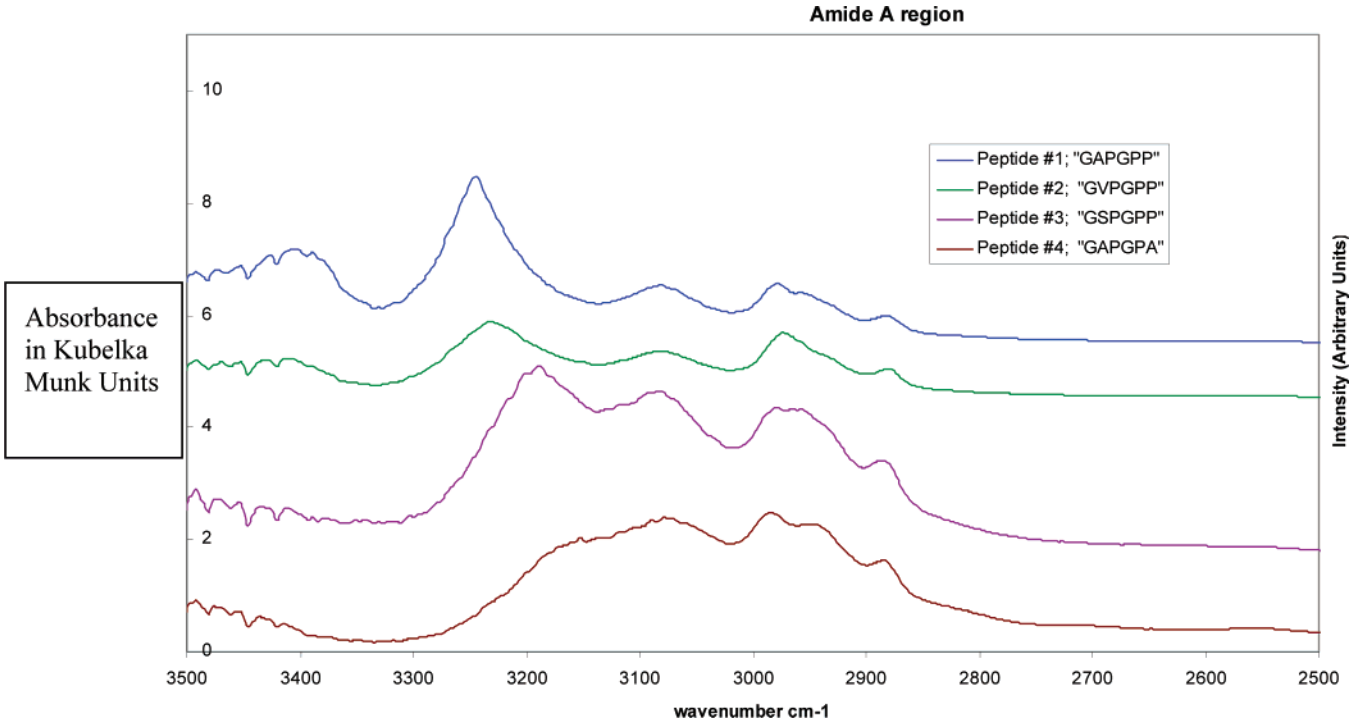

Figure 6. Infrared spectra for peptides **1**−**4** (from top to bottom), in the triple helix conformation and supercoiling-sensitive amide A band region. Wavenumbers are in cm^{-1}. All of the absorbances are characteristic of the model peptides in the triple helical state,[9] corroborating the X-ray diffraction results.

with surface features less than 50−100 nm, suggesting that surface tension during drying exerts a considerable surface smoothing effect.

The major objective of the current study was to look for correlations between the periodicity observed on the micron scale and peptide sequence, molecular shape, and packing geometry on the nanoscale. There are two current explanations of the role that molecular level features have in determining features of a chiral mesophase that approach the macroscopic scale. The first of these was a theory advanced by Rudall[10,48] to explain the fit between chitin and collagen in certain tissues in terms of bulges and grooves in the helical molecules. This idea of a geometric fit between molecules was extrapolated to explain the twisted helicoids observed for many biological materials comprised of helical molecules. However, cholesteric periods calculated from the pitch induced by helix−helix fits are of the wrong order of magnitude. In addition a simple "bulge to groove" model does not explain the differences in *cholesteric material pitch*, which we observe for molecules in identical conformations—with identical *molecular helix* pitches. A more comprehensive, though not necessarily contradictory, description was recently advanced by Harris, Kamien, and Lubensky.[49−51] In essence, they state that a chiral parameter contributes to the free energy of the cholesteric and is determined by the overall "biaxiality" of the molecule. The pitch of a cholesteric mesophase depends on the biaxiality of the mesogen, in this case a helical molecule, where more biaxial (oblate cross section, as illustrated in Figure 7a) molecules are more strongly chiral. In both descriptions, a correlation between conformation and chirality is also expected.

Using the crystallographic data for the molecules in the periodically banded solids we can easily obtain an experimental measure of the conformation using the rise per amino acid; observed as a moderately strong reflection in the X-ray powder diagrams. The peptides used in the current study encompass only very subtle differences in conformation (all are triple helical, after all) and possess fairly large differences in chiral side chain "decorations" along the helix which we would expect to overwhelm any contribution due to conformation. The packing of the molecules within a crystalline unit cell can be viewed as an experimental measure of their "biaxiality". However the packing of molecules in a crystal is determined by a number of different factors, including electrostatic, hydrogen bonded interactions, and possibly bound water in addition to the geometry of the molecule (nonpolar van der Waals forces). Any apparent packing features suggestive of biaxiality thus are a combination of the shape of the molecule and the "shape" of its interaction with its surroundings. Cylindrical, molecules with a nonchiral cross-section will pack hexagonally, with all nearest neighbor distances equal. Deviations from hexagonal packing, where γ is no longer equal to 120°, indicate that the molecules pack with nonequivalent nearest neighbor distances, as shown in Figure 7b. These deviations can can be calculated from the unit cell parameters, and can thus be viewed as an experimental measure of effective molecular biaxiality.

Crystallographic Packing and Banded Pattern. The periodicities observed on the surfaces are strongly correlated to the packing asymmetry for all four peptides (Table 5), with the most chiral cross sections corresponding to the shortest period for the banded pattern on the material surface. These results lend qualitative support to Harris, Kamien, and Lubensky's description,[50,51] which predicts shorter cholesteric periods for molecules with more asymmetric cross sections.

The inequality between nearest neighbor packing directions can also be expressed simply as the ratio of nearest neighbor distances. In a two-chain orthorhombic unit cell this is the ratio between the 110 spacing and either the 100 or 010 spacing (whichever is shorter). In

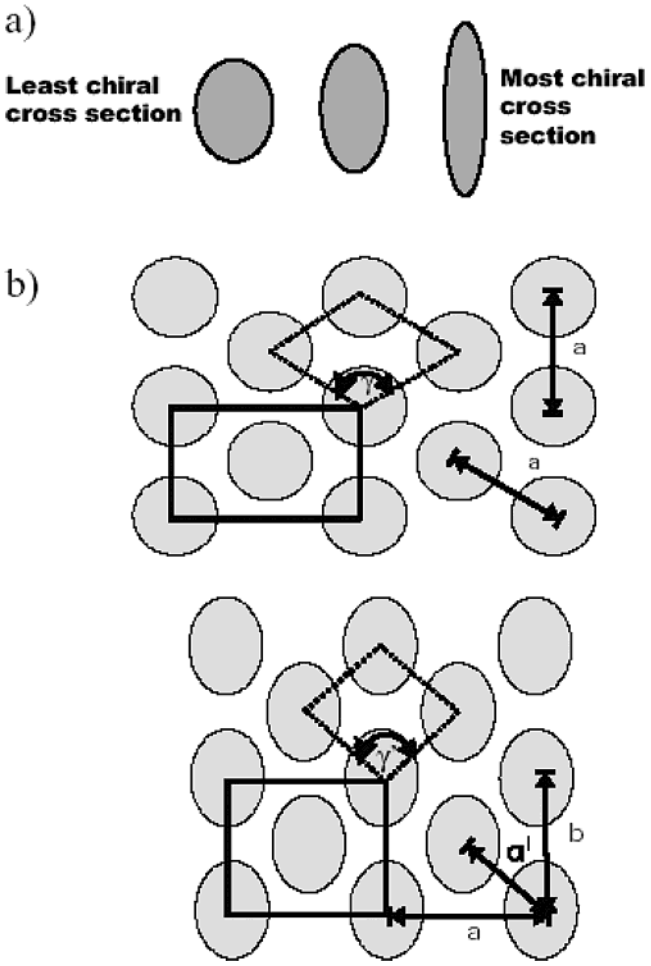

Figure 7. Schematics showing the relationship between the molecular chirality defined by Harris Kamien and Lubensky[50,51] and the basal plane crystalline packing of approximately cylindrical molecules. (a) Cross section of a molecule is a major determinant of chirality, where a circular cross section is less chiral than an elliptical cross section. (b) In a pseudohexagonal packing of cylindrical molecules, the angle between chains (defined in the figure as γ) is approximately 120°, and nearest neighbor distances (a in the figure) are approximately equal (top). If the cylinders are slightly distorted so that their cross sections begin to look elliptical, the nearest neighbor spacings are no longer equal (a and a') and the angle between chains (γ) is no longer 120° (bottom). In both cases an orthorhombic or monoclinic unit cell can be defined to incorporate two chains.

Figure 7b, these are the b (0 1 0) and a' (1 1 0) dimensions in the deformed nonhexagonal unit cell shown at the bottom. There is a correlation between banded period and ratio of nearest neighbor distances, which appears to be approximately linear for all of the peptide materials where the peptides adopt the same triple helical conformation, the 10/3 helix having a 2.95 Å rise per amino acid (Figure 8). The shorter more cylindrical conformation exhibited by GAPGPP follows

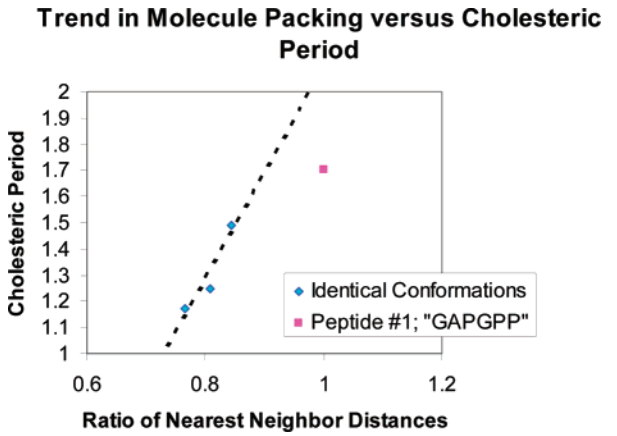

Figure 8. Graphical representation for the trend correlating molecular packing asymmetry with surface pattern periodicity can be constructed by comparing the ratio of nearest neighbor distances (1 for hexagonal, d_{110}/d_{100} for orthorhombic structures). The peptides (**2**, **3**, **4**) with the same triple helical conformation can all be fit with the same line, but peptide **1** (with a different conformation) does not quantitatively fit this trend. There thus may be a contribution due to overall length of the triple helical rod (shortened in a more supercoiled triple helical conformation) and the helix symmetry (conformation) in the relationship between molecular structure and surface texture periodicity.

the same qualitative trend of increasing surface pattern periods for helices with a more cylindrical cross section but does not quantitatively fit the trend predicted by the 10/3 triple helical peptides and resulting materials. The surface periodicity of this peptide is shorter than predicted from the trend produced by the other peptides, indicating an additional subtle contribution from the shorter helix conformation or overall shorter length of the triple helical "rod" in this conformation.

Conclusions

The collagen glassy surfaces studied feature chemical as well as topographic periodic patterns as a result of the blocky structure of the collagen model oligopeptides and their chiral "liquid" crystalline arrangement. This ability to pattern the surface and interior surfaces of a material is expected to be quite general—to include chemical patterns, written into the side chain pattern, that encompass chemical features other than hydrophobicity/hydrophilicity. Thus, lyotropic rodlike chiral liquid crystals with a blocky structure can be used as a general approach to fabricate biopolymeric materials with repetitive micron and submicron scale surface chemistry and topographic patterns. These features are expected to be engineerable, because sequence specific periodic features are observed in glassy solids of collagen-like oligopeptides. The periodicity of the features qualitatively agrees with chirality predictions based on molecular shape and steric interactions. It is not unreasonable to expect that prediction of collagen glassy solid features

Table 5. Effective Angle between Chains in the Peptide Films, γ, Compared to the Periodicities of Cholesteric-Like Patterns Observed on the Film Surfaces[a]

oligopeptide triple helical sequence	rise per amino acid, Å	helix symmetry	effective angle between chains, deg	"cholesteric" band spacing, μm
1: "GAPGPP"	2.67	4/1 (left-handed 4-fold)	120 (cylinders)	1.70
2: "GAPGPA"	2.95	10/3 (left-handed 3.3-fold)	114.9	1.49
3: "GVPGPP"	2.95	10/3 (left-handed 3.3-fold)	107.9	1.25
4: "GSPGPP"	2.95	10/3 (left-handed 3.3-fold)	101.7	1.17

[a] The angle γ is calculated as arctan(d_{110}/d_{100}).

from molecular structure (sequence) and from processing environment (temperature, concentration) will be possible as more data are amassed.

Acknowledgment. We thank NASA and the Air Force for support of this work. The authors would like to acknowledge useful discussions with Thieu Vuong, David Knight, Christopher Viney and Jun Magoshi. Suggestions and facilities support from Edward Atkins, Helmut Strey, and Alan Wadden are also gratefully acknowledged.

References and Notes

(1) Li, M. H.; Fan, P.; Brodsky, B.; Baum, J. *Biochemistry* **1993**, *32*, 7377−7387.
(2) Long, C. G.; Braswell, E.; Zhu, D.; Apigo, J.; Baum, J.; Brodsky, B. *Biochemistry* **1993**, *32*, 11688−11695.
(3) Bella, J.; Eaton, M.; Brodsky, B.; Berman, H. M. *Science* **1994**, *266*, 75−81.
(4) Shah, N. K.; Ramshaw, J. A.; Kirkpatrick, A.; Shah, C.; Brodsky, B. *Biochemistry* **1996**, *35*, 10262−10268.
(5) Brodsky, B.; Ramshaw, J. A. *Matrix Biol.* **1997**, *15*, 545−554.
(6) Feng, Y.; Melacini, G.; Goodman, M. *Biochemistry* **1997**, *36*, 8716−8724.
(7) Melacini, G.; Feng, Y.; Goodman, M. *Biochemistry* **1997**, *36*, 8725−8732.
(8) Beck, K.; Brodsky, B. *J. Struct. Biol.* **1998**, *122*, 17−29.
(9) Valluzzi, R.; Kaplan, D. L. *Biopolymers* **2000**, *53*, 350−362.
(10) Rudall, K. M. In *Treatise on Collagen*; Gould, B. S., Ed.; Academic Press: London, 1968; Vol. 2, Part A, pp 83−137.
(11) Ramachandran, G. N.; Doyle, B. B.; Blout, E. R. *Biopolymers* **1968**, *6*, 1771−1775.
(12) Andreva, N. S.; Esipova, N. G.; Millionova, M. I.; Rogulenkova, V. N.; Shibnev, V. A. In *Conformation of Biopolymers*, 1st ed.; Ramachandran, G. N., Ed.; Academic Press: New York, New York, 1967; Vol. 2, p 785.
(13) Rich, A.; Crick, F. H. C. *Nature (London)* **1955**, *176*, 915−916.
(14) Segal, D. M.; Traub, W.; Yonath, A. *J. Mol. Biol.* **1969**, *43*, 519−527.
(15) Traub, W. *J. Mol. Biol.* **1969**, *43*, 479−485.
(16) Yonath, A.; Traub, W. *J. Mol. Biol.* **1969**, *43*, 461−477.
(17) Shibnev, V. A.; Khalikov, S. K.; M. P, F.; Poroshin, K. T. *Izv. Akad. Nauk SSSR, Ser Khim.* **1970**, *1970*, 2822−2823.
(18) Hulmes, D. J.; Miller, A.; Parry, D. A.; Piez, K. A.; Woodhead-Galloway, J. *J. Mol. Biol.* **1973**, *79*, 137−148.
(19) Johnson, B. J. *J. Pharm. Sci.* **1974**, *63*, 313−327.
(20) Doyle, B. B.; Hukins, D. W.; Hulmes, D. J.; Miller, A.; Woodhead-Galloway, J. *J. Mol. Biol.* **1975**, *91*, 79−99.
(21) Miller, A. Molecular Arrangement in Collagen. *Ital. J. Biochem.* **1975**, *24* (1), 57−58.
(22) Scatturin, A.; Tamburro, A. M.; DelPra, A.; Bordignon, E. *Int. J. Pept. Protein Res.* **1975**, *7*, 425−435.
(23) Walton, A. G. *Colston Pap.* **1975**, *26*, 139−150.
(24) Hulmes, D. J.; Miller, A.; Parry, D. A.; Woodhead-Galloway, J. *Biochem. Biophys. Res. Commun.* **1977**, *77*, 574−580.
(25) Traub, W.; Yonath, A.; Segal, D. M. *Nature (London)* **1969**, *221*, 914−917.
(26) Segal, D. M.; Traub, W. *J. Mol. Biol.* **1969**, *43*, 487−496.
(27) Doyle, B. B.; Traub, W.; Lorenzi, G. P.; Blout, E. R. *Biochemistry* **1971**, *10*, 3052−3060.
(28) Okuyama, K.; Nagarajan, V.; Kamitori, S. *Proc. Indian Acad. Sci.-Chem. Sci.* **1999**, *111*, 19−34.
(29) Bella, J.; Brodsky, B.; Berman, H. M. *Structure* **1995**, *3*, 893−906.
(30) Bella, J.; Eaton, M.; Brodsky, B.; Berman, H. M. *Science* **1994**, *266*, 75−81.
(31) Martin, R.; Farjanel, J.; Eichenberger, D.; Colige, A.; Kessler, E.; Hulmes, D. J. S.; Giraud-Guille, M. M. *J. Mol. Biol.* **2000**, *301*, 11−17.
(32) Lepescheux, L. *Biol. Cell* **1988**, *62*, 17−31.
(33) Bouligand, Y.; Denefle, J. P.; Lechaire, J. P.; Maillard, M. *Biol. Cell* **1985**, *54*, 143−162.
(34) Gaill, F.; Herbage, D.; Lepescheux, L. *Matrix* **1991**, *11*, 197−205.
(35) Giraud-Guille, M. M. *Int. Rev. Cytol.* **1996**, *166*, 59−101.
(36) Besseau, L.; Giraud-Guille, M. M. *J. Mol. Biol.* **1995**, *251*, 197−202.
(37) Gathercole, L. J.; Barnard, K.; Atkins, E. D. *Int. J. Biol. Macromol.* **1989**, *11*, 335−338.
(38) Barnard, K.; Gathercole, L. J. *Int. J. Biol. Macromol.* **1991**, *13*, 359−365.
(39) Lees, S. *Biophys. J.* **1998**, *75*, 1058−1061.
(40) Woodhead-Galloway, J.; Knight, D. P. *Proc. R. Soc. London, B: Biol. Sci.* **1977**, *195*, 355−364.
(41) Knight, D. P.; Hunt, S. *Nature (London)* **1974**, *249*, 379−380.
(42) Knight, D. P.; Hunt, S. *Tissue Cell* **1976**, *8*, 183−193.
(43) Hukins, D. W. *J. Theor. Biol.* **1978**, *71*, 661−667.
(44) Hukins, D. W.; Woodhead-Galloway, J. *Biochem. Soc. Trans.* **1978**, *6*, 238−239.
(45) Gaill, F.; Lechaire, J. P.; Denefle, J. P. *Biol. Cell* **1991**, *72*, 149−158.
(46) Na, G. C.; Butz, L. J.; Bailey, D. G.; Carroll, R. J. *Biochemistry* **1986**, *25*, 958−966.
(47) Lubensky, T. C.; Tokihiro, T.; Renn, S. R. *Phys. Rev. A.* **1991**, *43*, 5449−5462.
(48) Rudall, K. M. Protein Ribbons & Sheets. *Lectures on the Scientific Basis of Medicine*; Athlone Press: London, 1956; Vol. 5, pp 217−230.
(49) Kamien, R. D. *Mol. Cryst. Liq. Cryst.* **2001**, *358*, 97−101.
(50) Harris, A. B.; Kamien, R. D.; Lubensky, T. C. *Phys. Rev. Lett.* **1997**, *78*, 1476−1479.
(51) Harris, A. B.; Kamien, R. D.; Lubensky, T. C. *Rev. Mod. Phys.* **1999**, *71*, 1745−1757.

MA0340659